

Existence And Distribution Of Limit Cycles In A Hamiltonian System*

Gheorghe Tigan†

Received 1 August 2005

Abstract

In this paper we study the existence, number and distribution of limit cycles of a perturbed Hamiltonian system. Applying the Abelian integral method [13] in the case $n = 4$ we can draw the distribution limit cycle diagrams.

1 Introduction

The system considered in this paper is a Hamiltonian system given by:

$$\begin{aligned}x' &= 4y(abx^2 - by^2 + 1) + \varepsilon x(ux^n + vy^n - b\frac{\beta+1}{\mu+1}x^\mu y^\beta - ux^2 - \lambda) \\y' &= 4x(ax^2 - aby^2 - 1) + \varepsilon y(ux^n + vy^n + bx^\mu y^\beta - vy^2 - \lambda)\end{aligned}\quad (1)$$

where $\mu + \beta = n$, $0 < a < b < 1$, $0 < \varepsilon \ll 1$, u, v, λ are the real parameters and $n = 2k$, k a positive integer. Some results on this system are reported in [8, 9] and on a related system in [10].

It is known that one way to produce limit cycles is by perturbing a Hamiltonian system which has one or more centers, in such a way that limit cycles bifurcate in the perturbed system from some of the periodic orbits in the original system. There are some methods in doing that. The first one is based on the Poincaré return map [4], the second on the Poincaré-Melnikov integral method [12], the third on the Abelian integral method [13] and the last is presented in [14]. In the plane, the first two are equivalent.

The following result is registered in [2].

THEOREM 1. Consider the perturbed Hamiltonian system

$$x' = -\frac{\partial H}{\partial y} + P(x, y, \alpha), y' = \frac{\partial H}{\partial x} + Q(x, y, \alpha).\quad (2)$$

Assume that P and Q are polynomials and $P(x, y, 0) = Q(x, y, 0) = 0$. The curve Γ^h defined by the Hamiltonian $H(x, y) = h$ of system (2) is a periodic orbit that extends

*Mathematics Subject Classifications: 34C07, 37G15.

†Department of Mathematics, "Politehnica" University of Timisoara, Pta Victoriei, No 2, 300006, Timisoara, Timis, Romania

outside as h increases, and $\Gamma^h(D)$ is the area inside Γ^h . If there exists h_0 such that function

$$A(h) = \iint_{\Gamma^h(D)} [P''_{x\alpha}(x, y, 0) + Q''_{y\alpha}(x, y, 0)] dx dy \quad (3)$$

satisfies $A(h_0) = 0$, $A'(h_0) \neq 0$, $\alpha A'(h_0) < 0$ (> 0), then system (2) has only one stable (unstable) limit cycle nearby Γ^{h_0} for α very small. If Γ^h constricts inside as h increases, the stability of the limit cycle is opposite with above. If $A(h) \neq 0$, then system (2) has no limit cycle.

The integral $A(h)$ is called the *Abelian integral* and the problem is known as the weakened 16-th Hilbert problem. If the form of the system (2) is:

$$\begin{cases} x'(t) = -\frac{\partial H}{\partial y} + \varepsilon x(p(x, y) - \lambda), \\ y'(t) = \frac{\partial H}{\partial x} + \varepsilon y(q(x, y) - \lambda) \end{cases} \quad (4)$$

where $p(0, 0) = q(0, 0) = 0$, then, by using the above Theorem 1, from $A(h) = 0$, we get:

$$\lambda = \lambda(h) = \frac{\iint_{\Gamma^h(D)} f(x, y) dx dy}{2 \iint_{\Gamma^h(D)} dx dy} \quad (5)$$

where $f(x, y) = xp'_x + yp'_y + p + q$.

This function $\lambda(h)$ is called *the detection function* of system (4).

From Theorem 1 and by using the detection function $\lambda(h)$ we get the following result.

PROPOSITION 1. Given λ_0 . a) If $(h_0, \lambda(h_0))$ is an intersecting point of line $\lambda = \lambda_0$ and the detection curve $\lambda = \lambda(h)$, and $\lambda'(h_0) > 0$ (< 0), then system (4) has only one stable (unstable) limit cycle nearby Γ^{h_0} when $\lambda = \lambda_0$. b) If line $\lambda = \lambda_0$ and the detection curve $\lambda = \lambda(h)$ have no intersecting point, then the system (4) has no limit cycle when $\lambda = \lambda_0$. If the Γ^h constricts inside as h increases, the stability of the limit cycle is opposite with above.

This paper is organized as follows. In Section 2, we describe the global portrait of the unperturbed system. In Section 3, we obtain the analytical forms of the detection functions. Then, using a Computer System Algebra, we get numerical results. Finally, we obtain the distribution of the limit cycles.

2 The Phase Portrait of the Unperturbed System

The unperturbed system (6) corresponding to system (1) is

$$\begin{cases} x' = 4y(-by^2 + bax^2 + 1) \\ y' = 4x(ax^2 - y^2ba - 1) \end{cases} \quad (6)$$

that is, system (1) in the case $\varepsilon = 0$. System (6) has nine finite singular points and they are

$$\begin{aligned}
& O(0,0), \\
& A_1 \left(\sqrt{\frac{1+a}{a(1-ba)}}, \frac{1}{b-b^2a} \sqrt{b(1-ba)(1+b)} \right), \\
& A_2 \left(\sqrt{\frac{1+a}{a(1-ba)}}, \frac{-1}{b-b^2a} \sqrt{b(1-ba)(1+b)} \right), \\
& A_3 \left(-\sqrt{\frac{1+a}{a(1-ba)}}, \frac{1}{b-b^2a} \sqrt{b(1-ba)(1+b)} \right), \\
& A_4 \left(-\sqrt{\frac{1+a}{a(1-ba)}}, \frac{-1}{b-b^2a} \sqrt{b(1-ba)(1+b)} \right), \\
& B_1 \left(0, \sqrt{\frac{1}{b}} \right), B_2 \left(0, -\sqrt{\frac{1}{b}} \right), \\
& C_1 \left(\sqrt{\frac{1}{a}}, 0 \right), C_2 \left(-\sqrt{\frac{1}{a}}, 0 \right).
\end{aligned}$$

By computing the eigenvalues at each singular point we may see that O, A_1, A_2, A_3, A_4 are centers while the other singular points B_1, B_2, C_1, C_2 are hyperbolic saddle points. Further the Hamiltonian of system (6) is

$$H(x, y) = -(ax^4 + by^4) + 2abx^2y^2 + 2(x^2 + y^2) = h \quad (7)$$

and $H(A_i) = \frac{2ba+b+a}{ba(1-ba)}$ for $i = 1, 2, 3, 4$, $H(B_k) = \frac{1}{b}$, $H(C_k) = \frac{1}{a}$ for $k = 1, 2$. Since $0 < a < b < 1$, we get that $H(O) < H(B_1) < H(C_1) < H(A_1)$.

In polar coordinates, $x = r \cos \theta, y = r \sin \theta$, system (6) becomes:

$$r' = -r^3 p'(\theta), \quad \theta' = -1 + r^2 p(\theta) \quad (8)$$

and the Hamiltonian (7) reads

$$H(r, \theta) = -r^4 p(\theta) + 2r^2 = h, \quad (9)$$

where

$$p(\theta) = a \cos^4 \theta + b \sin^4 \theta - 2ab \cos^2 \theta \sin^2 \theta. \quad (10)$$

REMARK 1. The equilibrium points A_1, A_2, A_3, A_4 lie on the lines $d_{\pm} : \theta = \pm \arccos \sqrt{\frac{b+ba}{a+b+2ab}}$

THEOREM 2. As h varies on the real line, the level curves defined by the Hamiltonian (9) can be divided as follows [8]:

1. $\Gamma_1^h : -\infty < h < 0$, this corresponds to an orbit that surrounds all critical points, fig.1 a).
2. $\Gamma_2^h \cup \Gamma_1^h : 0 \leq h < \frac{1}{b}$, this corresponds to an orbit (Γ_2^h) that surrounds only the origin and a curve of type (Γ_1^h), fig.1 b)-a).
3. $\Gamma_3^h : \frac{1}{b} < h < \frac{1}{a}$, this corresponds to two symmetric orbits that do not intersect the Oy axis but encircle the rest of critical points. If $h = \frac{1}{b}$ we get four heteroclinic orbits connecting the critical points B_1 and B_2 , fig.2 b)-a).
4. $\Gamma_4^h : \frac{1}{a} < h < \frac{2ba+b+a}{ba(1-ba)}$, this corresponds to four orbits that surround respectively the $A_i, i = 1, 2, 3, 4$, equilibrium points. If $h = \frac{1}{a}$ we have four homoclinic orbits connecting the critical points C_1 and C_2 , fig.3 b)-a). Note that as h increases, the curves Γ_1^h, Γ_3^h and Γ_4^h shrink inside, while Γ_2^h extends outside.

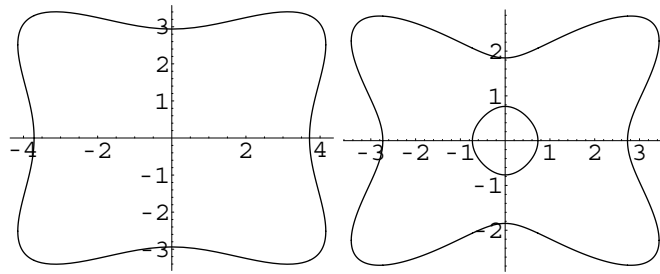


Figure 1: Orbit of type a) Γ_1 (left) b) Γ_2 and Γ_1 (right)

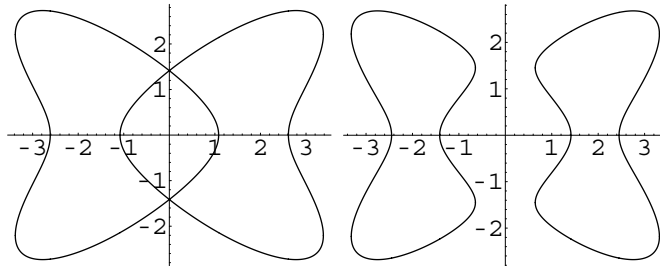


Figure 2: a) Four heteroclinic orbits connecting two critical points B_1 and B_2 (left) b) Two orbits of type Γ_3 (right)

3 Numerical Explorations

In this section we numerically compute the detection curves and the distribution of limit cycles. The four detection functions can be computed numerically, and for a given h , they depend on u and v , (see tables 1-4). On the other hand, for two given

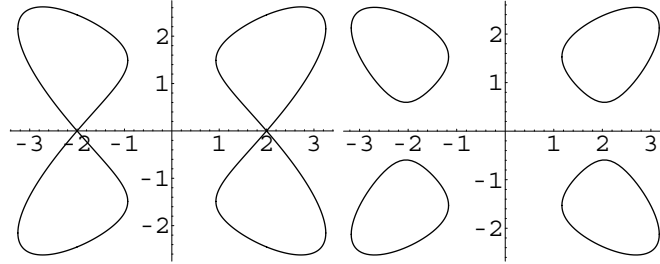


Figure 3: a) Four homoclinic orbits connecting the critical points C_1 and C_2 (left) b) Four orbits of type Γ_4 (right)

values of u and v , the detection curves can be drawn on the (h, λ) -plane, as illustrated in fig.4. By the Proposition 1 and the detection function graphs, the existence, number and distribution of limit cycles can then be obtained. We consider here the case $n = 4$ that means perturbation of five order.

From (9), we get

$$r_{1,2} = r_{\pm}^2(\theta, h) = \frac{1 \pm \sqrt{1 - hp(\theta)}}{p(\theta)} \quad (11)$$

and from $\theta' = -1 + r^2 p(\theta) = 0$ we have:

$$\begin{aligned} \theta_1(h) &= \frac{1}{2} \arccos \left[\left(b - a + 2\sqrt{a^2 b^2 - ab + (a + b + 2ab) h^{-1}} \right) / (a + b + 2ab) \right], \\ \theta_2(h) &= \frac{1}{2} \arccos \left[\left(b - a - 2\sqrt{a^2 b^2 - ab + (a + b + 2ab) h^{-1}} \right) / (a + b + 2ab) \right]. \end{aligned}$$

From the form of the perturbation terms

$$p(x, y) = x \left(ux^n + vy^n - b \frac{\beta + 1}{\mu + 1} x^\mu y^\beta - ux^2 \right), q(x, y) = y (ux^n + vy^n + bx^\mu y^\beta - vy^2)$$

we have

$$\frac{\partial^2 p(x, y)}{\partial x \partial \varepsilon} + \frac{\partial^2 q(x, y)}{\partial y \partial \varepsilon} = (2 + n)(ux^n + vy^n) - 3(ux^2 + vy^2) - 2\lambda.$$

Therefore, the four detection functions corresponding to the four closed curves Γ_j^h , $j = 1, 2, 3, 4$, for the above perturbations are

$$\lambda_j(h) = \frac{\iint_{\Gamma_j^h(D)} [(n + 2)(ux^n + vy^n) - 3(ux^2 + vy^2)] dx dy}{2 \iint_{\Gamma_j^h(D)} dx dy}, j = 1, 2, 3, 4. \quad (12)$$

In polar coordinates and for $a = \frac{1}{6}, b = \frac{1}{3}, n = 4$ (12) leads to:

$$\lambda_1(h) = \frac{\int_0^{2\pi} (r_1^3(\theta, h) g(\theta) - \frac{3}{4} r_1^2(\theta, h) g_1(\theta)) d\theta}{\int_0^{2\pi} r_1(\theta, h) d\theta}, \quad -\infty < h < 3, \quad (13)$$

$$\lambda_2(h) = \frac{\int_0^{2\pi} (r_2^3(\theta, h) g(\theta) - \frac{3}{4} r_2^2(\theta, h) g_1(\theta)) d\theta}{\int_0^{2\pi} r_2(\theta, h) d\theta}, \quad 0 < h < 3, \quad (14)$$

$$\lambda_3(h) = \frac{\int_{-\theta_2(h)}^{\theta_2(h)} [(r_1^3(\theta, h) - r_2^3(\theta, h)) g(\theta) - \frac{3}{4} (r_1^2(\theta, h) - r_2^2(\theta, h)) g_1(\theta)] d\theta}{\int_{-\theta_2(h)}^{\theta_2(h)} (r_1(\theta, h) - r_2(\theta, h)) d\theta} \quad (15)$$

$$3 < h < 6,$$

$$\lambda_4(h) = \frac{\int_{\theta_1(h)}^{\theta_2(h)} [(r_1^3(\theta, h) - r_2^3(\theta, h)) g(\theta) - \frac{3}{4} (r_1^2(\theta, h) - r_2^2(\theta, h)) g_1(\theta)] d\theta}{\int_{\theta_1(h)}^{\theta_2(h)} (r_1(\theta, h) - r_2(\theta, h)) d\theta} \quad (16)$$

$$6 < h < 11.647,$$

where $g(\theta) = u \cos^4 \theta + v \sin^4 \theta, g_1(\theta) = u \cos^2 \theta + v \sin^2 \theta$ and $r_{1,2}(\theta, h) = r_{\pm}^2(\theta, h)$.

From (13)-(16) we obtain values of detection functions $\lambda_i(h), i = 1, 2, 3, 4$, registered in the following tables (1-4).

Table 1. Values of detection function $\lambda_1(h)$ when $a = 1/6, b = 1/3, n = 4$.

h	$\lambda_1(h)$	h	$\lambda_1(h)$	h	$\lambda_1(h)$
-2	138.889 u + 49.363 v	-1.85	137.980 u + 48.939 v	-1.7	137.069 u + 48.514
-1.55	136.156 u + 48.087 v	-1.4	135.242 u + 47.660 v	-1.25	134.327 u + 47.231 v
-1.1	133.410 u + 46.802 v	-0.95	132.492 u + 46.371 v	-0.8	131.572 u + 45.939 v
-0.65	130.651 u + 45.505 v	-0.5	129.728 u + 45.070 v	-0.35	128.805 u + 44.634 v
-0.2	127.880 u + 44.197 v	-0.05	126.955 u + 43.758 v	0.1	126.028 u + 43.318 v
0.25	125.101 u + 42.877 v	0.4	124.173 u + 42.434 v	0.55	123.245 u + 41.990 v
0.7	122.317 u + 41.544 v	0.85	121.390 u + 41.097 v	1	120.463 u + 40.648 v
1.15	119.537 u + 40.198 v	1.3	118.613 u + 39.746 v	1.45	117.692 u + 39.293 v
1.6	116.773 u + 38.838 v	1.75	115.860 u + 38.382 v	1.9	114.952 u + 37.925 v
2.05	114.051 u + 37.466 v	2.2	113.162 u + 37.006 v	2.35	112.286 u + 36.545 v
2.5	111.431 u + 36.083 v	2.65	110.605 u + 35.622 v	2.8	109.827 u + 35.163 v
2.95	109.154 u + 34.711 v				

Table 2. Values of detection function $\lambda_2(h)$ when $a = 1/6, b = 1/3, n = 4$.

h	$\lambda_2(h)$	h	$\lambda_2(h)$	h	$\lambda_2(h)$
0.01	-0.001 u - 0.001 v	0.21	-0.035 u - 0.035 v	0.41	-0.061 u - 0.062 v
0.61	-0.079 u - 0.081 v	0.81	-0.090 u - 0.091 v	1.01	-0.092 u - 0.091 v
1.21	-0.086 u - 0.081 v	1.41	-0.07 u - 0.058 v	1.61	-0.046 u - 0.021 v
1.81	-0.012 u + 0.032 v	2.01	0.031 u + 0.107 v	2.21	0.085 u + 0.208 v
2.41	0.149 u + 0.343 v	2.61	0.224 u + 0.529 v	2.81	0.308 u + 0.800 v

Table 3. Values of detection function $\lambda_3(h)$ when $a = 1/6, b = 1/3, n = 4$.

h	$\lambda_3(h)$	h	$\lambda_3(h)$	h	$\lambda_3(h)$
3	128.849 u + 40.643 v	3.08	129.732 u + 40.683 v	3.16	130.340 u + 40.685 v
3.24	130.850 u + 40.673 v	3.32	131.298 u + 40.653 v	3.4	131.703 u + 40.627 v
3.48	132.073 u + 40.598 v	3.56	132.416 u + 40.565 v	3.64	132.737 u + 40.531 v
3.72	133.038 u + 40.495 v	3.8	133.322 u + 40.458 v	3.88	133.593 u + 40.421 v
3.96	133.851 u + 40.383 v	4.04	134.098 u + 40.347 v	4.12	134.335 u + 40.311 v
4.2	134.565 u + 40.276 v	4.28	134.787 u + 40.242 v	4.36	135.003 u + 40.211 v
4.44	135.214 u + 40.181 v	4.52	135.421 u + 40.155 v	4.6	135.624 u + 40.132 v
4.68	135.825 u + 40.112 v	4.76	136.025 u + 40.097 v	4.84	136.223 u + 40.086 v
4.92	136.422 u + 40.081 v	5.	136.623 u + 40.082 v	5.08	136.825 u + 40.090 v
5.16	137.032 u + 40.107 v	5.24	137.243 u + 40.132 v	5.32	137.462 u + 40.169 v
5.4	137.689 u + 40.218 v	5.48	137.927 u + 40.281 v	5.56	138.179 u + 40.362 v
5.64	138.45 u + 40.465 v	5.72	138.744 u + 40.594 v	5.8	139.071 u + 40.76 v
5.88	139.446 u + 40.976 v	5.96	139.908 u + 41.281 v	6	140.235 u + 41.532 v

Table 4. Values of detection function $\lambda_4(h)$ when $a = 1/6, b = 1/3, n = 4$.

h	$\lambda_4(h)$	h	$\lambda_4(h)$	h	$\lambda_4(h)$
6	140.235 u + 41.532 v	6.15	141.234 u + 42.244 v	6.3	141.977 u + 42.705 v
6.45	142.631 u + 43.082 v	6.6	143.227 u + 43.408 v	6.75	143.781 u + 43.697 v
6.9	144.301 u + 43.959 v	7.05	144.793 u + 44.199 v	7.2	145.260 u + 44.419 v
7.35	145.706 u + 44.624 v	7.5	146.133 u + 44.816 v	7.65	146.543 u + 44.995 v
7.8	146.936 u + 45.163 v	7.95	147.315 u + 45.321 v	8.1	147.680 u + 45.470 v
8.25	148.033 u + 45.612 v	8.4	148.373 u + 45.746 v	8.55	148.703 u + 45.872 v
8.7	149.021 u + 45.993 v	8.85	149.330 u + 46.107 v	9.	149.629 u + 46.216 v
9.15	149.918 u + 46.319 v	9.3	150.200 u + 46.418 v	9.45	150.472 u + 46.511 v
9.6	150.737 u + 46.600 v	9.75	150.994 u + 46.685 v	9.9	151.244 u + 46.766 v
10.05	151.486 u + 46.843 v	10.2	151.722 u + 46.916 v	10.35	151.951 u + 46.986 v
10.5	152.174 u + 47.052 v	10.65	152.390 u + 47.115 v	10.8	152.600 u + 47.175 v
10.95	152.805 u + 47.232 v	11.1	153.004 u + 47.286 v	11.25	153.198 u + 47.337 v
11.4	153.386 u + 47.385 v	11.55	153.568 u + 47.431 v	11.64	153.667 u + 47.455 v

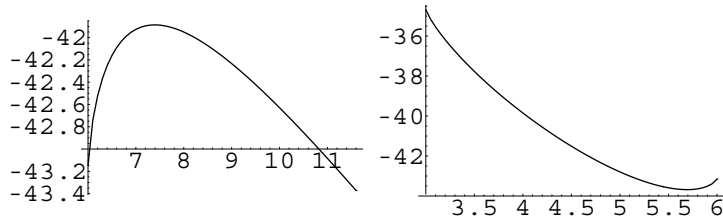


Figure 4: Detection curves λ_4 (left), λ_3 (right) of system (1) for $a = 1/6, b = 1/3, n = 4, u = -0.9$ and $v = 2$.

From tables (1-4) we have the four detection functions, two of which are shown in fig.4. The values of λ_1 and λ_2 are not plotted because they are outside the interval of the values of λ_3 and λ_4 . By using Proposition 1 and from fig.4 we have the following result.

THEOREM 3. For $a = 1/6, b = 1/3, n = 4, u = -0.9, v = 2$ and $0 < \varepsilon \ll 1$, we have that local maximum of λ_4 is -41.8864 , first point of λ_4 is -43.1473 , last point of λ_4 is -43.390 , local minimum of λ_3 is -43.679 , first point of λ_3 is -34.6781 , last point of λ_3 is -43.1473 . Based on these values we have:

a) $-43.679 < \lambda < -43.39$, system (1) has at least four limit cycles, two of which in the neighborhood of each orbit of type Γ_3^h , fig.5 a)

b) If $-43.39 < \lambda < -43.1473$, system (1) has at least eight limit cycles, two of which in the neighborhood of each orbit of type Γ_3^h and one in the neighborhood of the orbits of type Γ_4^h , fig.5 b)

c) If $-43.1473 < \lambda < -41.8864$, system (1) has at least ten limit cycles, two of which in the neighborhood of each orbit of type Γ_4^h and one in the neighborhood of the orbits of type Γ_3^h , fig.6 a)

d) If $-41.8864 < \lambda < -34.6781$, system (1) has at least two limit cycles, one of which in the neighborhood of each orbit of type Γ_3^h , fig.6 b).

From fig.4 we could obtain more results but we listed only these important cases.

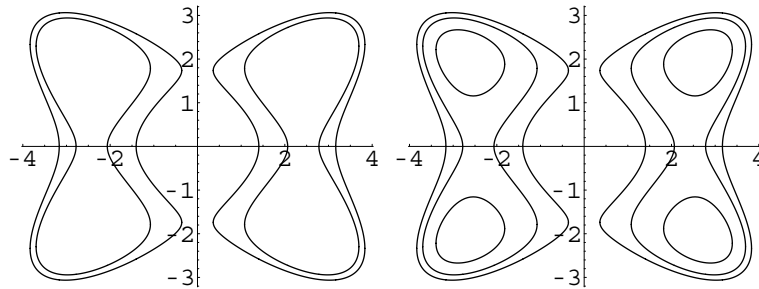


Figure 5: Distribution diagram corresponding to: a) four (left) b) eight (right) limit cycles of system (1).

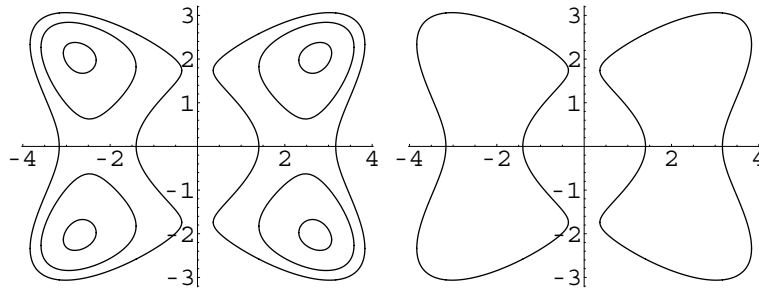


Figure 6: Distribution diagram corresponding to: a) ten (left) b) two (right) limit cycles of system (1).

4 Conclusions

System (1) with $a = \frac{1}{6}, b = \frac{1}{3}, n = 4, u = -0.9, v = 2, 0 < \varepsilon \ll 1$ and $-43.1473 < \lambda < -41.8864$, has at least ten limit cycles. The Abelian integral method was employed. By numerical explorations we have drawn the shape of the graphs of the detection functions from which we concluded about the number and distribution of limit cycles. A natural question is: one can obtain more limit cycles for higher perturbations?

Acknowledgements. This work was (partially) supported through a European Community Marie Curie Fellowship and in the framework of the CTS, contract number HPMT-CT-2001-00278.

References

- [1] J. B. Li and Z. R. Liu, Bifurcation set and limit cycles forming compound eyes in a perturbed Hamiltonian system, *Publ.Math.*, 35(1991), 487–506.
- [2] H. J. Cao, Z. G. Liu and Z. J. Jing, Bifurcation set and distribution of limit cycles for a class of cubic Hamiltonian system with higher-order perturbed terms, *Chaos, Solitons and Fractals* 11(2000), 2293–2304.
- [3] M. Y. Tang and X. C. Hong, Fourteen limit cycles in a cubic Hamiltonian system with nine-order perturbed term, *Chaos, Solitons and Fractals* 14(2002), 1361–1369.
- [4] S. N. Chow, C. Z. Li and D. Wang, *Normal Forms and Bifurcation of Planar Vector Fields*, Cambridge University Press, Cambridge, 1994.
- [5] Y. Q. Ye, S. L. Cai, L. S. Chen, K. C. Huang, D. J. Luo, Z. E. Ma, E. N. Wang, M. S. Wang, X. A. Yang, *Theory of limit cycles*, Translated from the Chinese by Chi Y. Lo. Second edition. *Translations of Mathematical Monographs*, 66. American Mathematical Society, Providence, RI, 1986.
- [6] C. F. Li and J. B. Li, Distribution of limit cycles for planar cubic Hamiltonian systems, *Acta Math Sinica*, 28(1985), 509–521.
- [7] J. B. Li and Q. M. Huang, Bifurcation of limit cycles forming compound eyes in the cubic system, *Chinese Ann. Math.*, 8B(4)(1987), 391–403.
- [8] Gh. Tigan, Thirteen limit cycles for a class of Hamiltonian systems under seven-order perturbed terms, *Chaos, Solitons and Fractals* (accepted), to appear.
- [9] Gh. Tigan, Analysis of a perturbed Hamiltonian system, in review.
- [10] Gh. Tigan, Eleven limit cycles in a Hamiltonian system, *The 5-th Conference of Balkan Society of Geometers*, Mangalia, 2005.
- [11] H. Giacomini, J. Llibre and M. Viano, On the nonexistence, existence and uniqueness of limit cycles, *Nonlinearity*, 9(1996), 501–516.

- [12] A. A. Andronov, Theory of bifurcations of dynamical systems on a plane, Israel program for scientific translations, Jerusalem, 1971.
- [13] T. R. Blows and L. M. Perko, Bifurcation of limit cycles from centers and separatrix cycles of planar analytic systems, *SIAM Rev.*, 36(1994), 341–376.
- [14] H. Giacomini, J. Llibre and M. Viano, On the shape of limit cycles that bifurcate from Hamiltonian centers, *Nonlinear Anal. Theory Methods Appl.*, 41(1997), 523–537.
- [15] Z. Hong, W. C. Chen, T. H. Zhang, Perturbation from a cubic Hamiltonian with three figure eight-loops, *Chaos, Solitons and Fractals*, 22(2004), 61–74.